

## Interactions between algal–bacterial populations and trace metals in fjord surface waters during a nutrient-stimulated summer bloom

*François L. L. Muller*<sup>1</sup>

Department of Chemistry, University of Bergen, Allégaten 41, 5007 Bergen, Norway

*Aud Larsen*

Department of Microbiology, University of Bergen, Jahnebakken 5, 5020 Bergen, Norway

*Colin A. Stedmon*

Department of Marine Ecology, National Environmental Research Institute, P.O. Box 358, Frederiksborgej 399, 4000 Roskilde, Denmark

*Morten Søndergaard*

Freshwater Biological Laboratory, University of Copenhagen, Helsingørsgade 51, 3400 Hillerød, Denmark

### Abstract

We examined how variations in algal–bacterial community structure relate to Cu, Zn, and Mn speciation during a diatom-rich bloom that was induced by daily additions of inorganic macronutrients to fjord waters in August 2002. The experiments were carried out in 11-m<sup>3</sup> floating mesocosm bags deployed in the Raunefjord, near Bergen, Norway, and operated in a chemostat (flow-through) mode. Copper speciation was controlled by the formation of very strong organic complexes ( $\log K'_1 = 15.2\text{--}15.8$ ;  $\log K'_2 = 13.0\text{--}13.4$ ) whose likely source was the cyanobacterium *Synechococcus* sp. Strong ligand concentrations were comparable to dissolved Cu levels. This covariation kept the free Cu<sup>2+</sup> concentration within the range of 10<sup>-12.4</sup> to 10<sup>-11.2</sup> mol L<sup>-1</sup>, i.e., below the toxicity threshold for *Synechococcus*. Weaker ligands ( $\log K'_3 = 8.2\text{--}9.4$ ) were released during—and up to 4 d following—the exponential growth of algae. During this period, the weaker Cu-binding ligands appeared to have the same source or production process as the proteinlike fluorophores detected in these coastal waters. Zinc speciation was controlled by complexation with a single class of organic ligands that appeared to be released inadvertently upon the death and/or grazing of phytoplankton. Labile manganese fluctuations were inversely synchronized with the abundance of heterotrophic bacteria until the coastal waters experienced a massive rain event on day 17 of the experiment. The rainfall, which was a source of nitrogen and micronutrients, appeared to stimulate the growth of larger cells (diatoms) but to inhibit that of the smaller cells (heterotrophic bacteria and cyanobacteria).

Trace elements such as Cu, Zn, and Mn perform essential biochemical functions within prokaryotic and eukaryotic cells (Whitfield 2001). The acquisition of these elements by the algal and bacterial cells present in seawater depends in part on the chemical forms in which they occur (Hudson and Morel 1993) and in part on the strategies used by the cells to optimize the uptake of essential elements (Riebesell and Wolf-Gladrow 2002) or minimize the ingress of potentially toxic ones. Thus, phytoplankton and bacteria are not only influenced by the availability of trace elements, but they also actively alter the composition of their environment to opti-

mize the use of these elements. It is important to note, however, that such feedbacks do not necessarily operate for the greater good of all algal and bacterial cells present. For example, small and large cells have different metal requirements due to the different diffusional paths involved in the supply of macro- and micronutrients to the cell surface (Riebesell and Wolf-Gladrow 2002). Secondly, the nature of the ligands released by a given phytoplankton species to bind a metal can act directly on the growth of another phytoplankton species (Vasconcelos et al. 2002). For these reasons, it is clear that trace metals potentially play a role in regulating the structure of the marine ecosystem.

Most studies of trace metal–phytoplankton interactions have been conducted in small-volume culture media in the laboratory. Typically, an artificial, sterilized, or filtered seawater medium would be inoculated with a unialgal culture, and the metal concentration or speciation would be controlled—either over time in the same culture or between different cultures. To understand the impact of trace metals on the structure of the phytoplankton community, however, there is clearly a need for more realistic investigations that include the whole microbial food web in a setting as close to the natural conditions as possible. One investigation of

<sup>1</sup> Corresponding author. Present address: Environmental Research Institute, Castle Street, Thurso KW14 7JD, Great Britain (francois.muller@thurso.uhi.ac.uk).

### Acknowledgments

We gratefully acknowledge the many good and insightful comments provided by our two anonymous reviewers, and we thank our Associate Editor (Mary I. Scranton) for pointing out a flaw in our original conclusions. This work was funded by an EU grant to M.S. (DOMAINE Project—contract HPRI-CT-2002-00181). The FACS-Calibur flow cytometer was funded in part by a grant from the Knut and Alice Wallenberg Foundation.

this type was carried out in June 2000 at the EU Large Scale Facility near Bergen, Norway (Muller et al. 2003). The 11-m<sup>3</sup> mesocosms were deployed in the Raunefjord alongside a large raft that was moored 200 m offshore. This mesocosm unit was particularly well suited to a time series investigation of metal speciation conducted in concert with a study of algal–bacterial bloom dynamics. One significant difference between the previous experimental setup and the present one, however, was that, in the earlier study, the bags were filled with fjord water at the beginning of the experiment, but the water was not renewed thereafter. One likely consequence of the closed system approach was that the concentrations of weak Cu-binding ligands declined rapidly with the increasing age of the water inside the bags (Muller et al. 2003), probably due to the isolation of the water from the source of these ligands.

The goal of the present study was to examine the effects of sustained biological activity, as occurred in August 2002, on the chemical speciation of Cu, Zn, and Mn in the above-mentioned fjord. Through controlled additions of silicate, we hoped to encourage a diatom bloom. The experiment was run in a chemostat mode, i.e., with a slow but continuous flow of water from the fjord to the bags that led to a hydraulic renewal rate of 10% per day. The most notable difference with the previous mesocosm experiment was the greater abundance of picoplankton (especially *Synechococcus* sp.) and Cu-binding ligands (especially high-affinity ligands) observed in August 2002 by comparison with June 2000. Finally, an exceptional rain event, which occurred on day 17 of the experiment, gave us the opportunity to examine the effects of a pulse in nitrogen and micronutrients on the abundance of each of the major groups of fjord-resident phytoplankton and bacteria. Small cells (cyanobacteria and heterotrophic bacteria) and large cells (diatoms) responded differently to the rain event. Picoplankton abundance decreased for 3 d, presumably due to their low tolerance for Cu (Moffett et al. 1997). By contrast, a transient bloom of diatoms, which were N limited in the fjord and in the bags at the time, occurred within 1 d of the rain event.

## Methods

**Study site and experimental setup**—The study took place in a Norwegian fjord (Raunefjord) situated 18 km south-southwest of Bergen and linked to a fjordic system running north to south between the mainland and the island of Sotra (Fig. 1). Ten large enclosures made of heavy-duty polyethylene (90% transmission of photosynthetic active radiation) were mounted on floating frames. The latter were secured alongside the upwind, south-facing side of a large raft that had been moored at a fixed location 200 m from the shore since the early 1990s. The polyethylene bags were rigorously cleaned with detergent prior to equilibration with seawater for 2 d. They were subsequently filled with 11 m<sup>3</sup> of fjord water, which was kept homogeneous by means of an airlift system (for details, see Egge and Aksnes 1992), and a small but uninterrupted flow of water from the fjord provided a hydraulic renewal of 10% per day throughout the experiment. The experiment presented took place in the last three

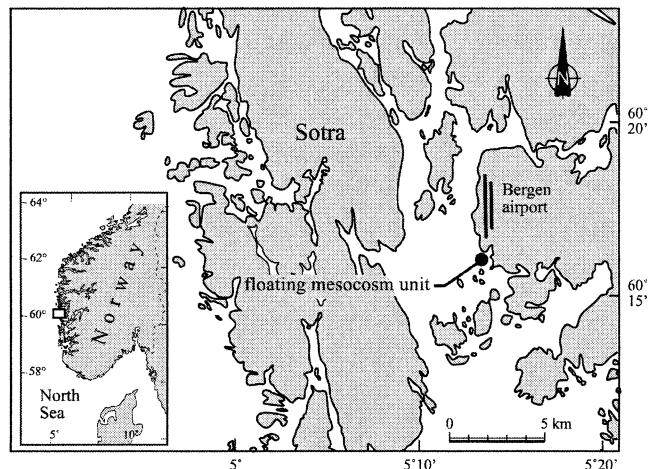


Fig. 1. Map of the study area showing the location of the floating mesocosm unit (filled circle) in the eastern part of Raunefjord.

enclosures (bags 8–10) as part of a wider study of organic matter production and fate in coastal ecosystems. Bag 8 was supplied daily with nitrate ( $\text{NaNO}_3$ , Merck Suprapur), phosphate ( $\text{K}_2\text{HPO}_4$ , Merck Suprapur), and silicate ( $\text{Na}_2\text{SiO}_3 \cdot 5 \text{H}_2\text{O}$ , BDH AnalaR) in molar Si:N:P ratios of 26:16:1 ( $2.6 \mu\text{mol L}^{-1} \text{Si}$ ;  $1.6 \mu\text{mol L}^{-1} \text{N}$ ; and  $0.1 \mu\text{mol L}^{-1} \text{P}$ ). Bags 9 and 10 received the same doses of silicate and nitrate as bag 8 but received larger doses of phosphate ( $0.2 \mu\text{mol L}^{-1} \text{P}$  and  $0.4 \mu\text{mol L}^{-1} \text{P}$ , respectively) during the last 2 weeks. The experiment was designed to induce increasingly N-deficient growth regimes of the plankton from bags 8–10 while keeping the total biomass unchanged, provided that growth was balanced at the Redfield ratio and that fjord water contained bioavailable forms of N and P in this ratio. However, both assumptions turned out to be incorrect. First, the plankton took up what they were given, irrespective of the N:P stoichiometry (Williams pers. comm.). Secondly, fjord waters turned out to be N deficient relative to P (Table 1). The overall consequence was that bags 8–10 were all equally limited by the availability of N. The identical state of N limitation in each of the bags led to nearly identical dissolved metal concentrations and speciation patterns. In short, trace metal chemistry was unaffected by the N:P dosing scheme. For these reasons, we are describing only those features that were common to all three bags, i.e., treating the latter as if they were essentially three replicates.

**Water quality parameters**—As a precaution against metal and organic contamination, no instrumentation was deployed at any time inside the bags. For example, temperature was measured only in the adjacent fjord, while salinity (S) was measured in the laboratory, in both cases with the help of an environmental probe model YSI 30 (Ocean Scientific). Water samples for inorganic nutrients, dissolved organic matter (DOM), and algal–bacterial numbers were taken from a depth of 1 m with a clean pumping system that consisted of (1) an Exide 12-V 70-Ah battery, (2) a Masterflex L/S drive combined with an Easy-Load pump head, and (3) a Tygon flexible tubing deployed with a boom over the side of the bag. Inorganic nutrients were analyzed by standard

Table 1. Inorganic nutrient concentrations recorded in bags 6–10 and in the fjord during the mesocosm experiment. ND, not determined.

(μmol L <sup>-1</sup> )					(μmol L <sup>-1</sup> )				
Day	Si(OH) <sub>4</sub>	PO <sub>4</sub>	NO <sub>3</sub> + NO <sub>2</sub> + NH <sub>4</sub>	N:P	Day	Si(OH) <sub>4</sub>	PO <sub>4</sub>	NO <sub>3</sub> + NO <sub>2</sub> + NH <sub>4</sub>	N:P
Raunefjord, depth = 6 m					Bag 8, depth = 2 m				
1	0.23	0.08	0.16	2.0	1	1.72	0.12	0.41	3.4
3	0.36	0.10	0.31	3.1	3	3.97	0.11	0.35	3.2
5	0.35	0.10	0.40	4.0	5	5.36	0.12	0.33	2.8
7	0.34	0.11	0.31	2.8	7	7.02	0.14	0.38	2.7
9	0.44	0.03	0.42	14.0	9	5.34	0.13	0.20	1.5
11	0.46	0.07	0.31	4.4	11	3.46	0.08	0.44	5.5
13	0.41	0.07	0.35	5.0	13	2.22	0.17	0.45	2.6
15	0.45	0.09	0.42	4.7	15	1.83	0.07	0.43	6.1
17	0.36	0.01	0.77	77.0	17	1.74	0.04	0.46	11.5
19	0.50	0.03	0.39	13.0	19	1.60	0.06	0.34	5.7
21	0.45	0.20	0.40	2.0	21	1.68	0.10	0.28	2.8
Bag 6, depth = 2 m					Bag 9, depth = 2 m				
1	1.64	0.10	0.43	4.3	1	1.73	0.10	0.40	4.0
3	4.21	0.11	0.28	2.5	3	3.63	0.11	0.28	2.5
5	6.49	0.12	0.26	2.2	5	5.05	0.12	0.32	2.6
7	8.14	0.14	0.29	2.1	7	6.31	0.15	0.20	1.3
9	5.36	0.06	0.21	3.5	9	4.24	0.06	0.16	2.6
11	1.28	0.08	0.57	7.1	11	2.38	0.09	0.51	5.7
13	0.29	0.09	0.52	5.8	13	1.14	0.09	0.27	3.0
15	0.21	0.10	0.83	8.3	15	1.03	0.11	0.42	3.8
17	0.49	0.02	1.08	54.0	17	0.86	0.04	0.46	11.5
19	0.81	ND	1.51	ND	19	0.86	0.04	0.33	8.2
21	0.78	ND	2.32	ND	21	0.91	0.12	0.31	2.6
Bag 7, depth = 2 m					Bag 10, depth = 2 m				
1	1.67	0.11	0.38	3.5	1	1.41	0.08	0.38	4.7
3	4.59	0.15	0.28	1.9	3	4.31	0.11	0.24	2.2
5	5.97	0.12	0.30	2.5	5	5.98	0.13	0.28	2.1
7	7.08	0.14	0.22	1.6	7	6.73	0.15	0.27	1.8
9	4.46	0.06	0.23	3.8	9	3.68	0.07	0.17	2.4
11	1.55	0.09	0.55	6.1	11	1.02	0.11	0.42	3.8
13	0.46	0.08	0.31	3.9	13	0.29	0.12	0.28	2.3
15	0.32	0.09	0.39	4.3	15	0.43	0.16	0.21	1.3
17	0.42	0.03	0.41	13.7	17	0.37	0.12	0.27	2.2
19	0.33	ND	0.36	ND	19	0.31	0.13	0.30	2.3
21	0.34	ND	0.38	ND	21	0.45	ND	0.28	ND

flow injection analysis procedures adapted to a Skalar SAN<sup>++</sup> automated segmented flow analyzer. Chlorophyll pigments, including chlorophyll *a* (Chl *a*), were determined from fluorescence emission measurements after extraction in methanol and high-pressure liquid chromatographic separation of the complex pigment mixture. Samples for pH and alkalinity (Alk) were stored in a cool box for no longer than 2 h prior to analysis. Measurements of pH<sub>NBS</sub> at 25°C were made on a Metrohm Model 713 pH meter using a Metrohm combined pH glass electrode and Aldrich reference buffers (pH 10.00, 7.00, and 4.00 at 25°C). These raw pH<sub>NBS</sub> values were later converted to the seawater scale (pH<sub>SWS</sub>) on the basis of total hydrogen ion concentrations. The conversion factors were obtained after performing a series of HCl titrations in artificial seawater samples. Total Alk was determined by potentiometric titration of seawater in a custom-built cell.

*Enumeration of phytoplankton and bacteria*—Autotrophic pico- and nanoeukaryotes, cyanobacteria, and heterotrophic

bacteria were determined by flow cytometry. All flow cytometric analyses were performed with a FACSCalibur flow cytometer (Becton Dickinson) equipped with an air-cooled laser providing 15 mW at 488 nm and with a standard filter setup. For algal counts, fresh samples were analyzed for 150–300 s. Enumeration of bacteria was performed on samples fixed with glutaraldehyde. Samples were analyzed for 60 s at event rates between 100 and 1,000 counts per second. Each sample was prepared at two different dilutions ranging from 10- to 200-fold before it was stained with SYBR Green I. The flow cytometer instrumentation and the attendant methodology followed the recommendations of Marie et al. (1999) and are described in more detail, for a similar study, by Larsen et al. (2001). Larger cells such as diatoms were identified and counted using a phase-contrast microscope (Jacquet et al. 2002).

*Characterization of the fluorescent fraction of DOM by three-dimensional excitation emission matrix spectroscopy*—The fluorescence of DOM in the fjord and that produced

in the bags was measured daily on GF/F-filtered samples using a Varian Eclipse fluorescence spectrophotometer. A series of emission scans (300–600 nm) were performed over a range of excitation wavelengths (240–450 nm), and the data were combined into a 3D-Excitation-Emission Matrix (EEM). The EEMs were Raman calibrated and corrected for excitation and emission instrument biases using the techniques described by Stedmon et al. (2003). The EEMs were characterized using parallel factor analysis (PARAFAC) (Stedmon et al. 2003). PARAFAC identified seven independent fluorescing groups in the DOM pool, five with fluorescence characteristics similar to humic material and two with proteinlike fluorescence (Stedmon and Markager pers. comm.).

*Sampling and handling procedures for trace metals*—Samples for pH, Alk, and trace metal analyses were taken at 2-m depth using a 4-liter low-density polyethylene (LDPE) bottle held in place along a Kevlar line and a plastic-coated bottom weight. They were brought to the shore-based laboratory within 45 min of collection. Separation of the suspended particulate matter (SPM) prior to both Alk and “dissolved” metal determinations was achieved by gentle pressure filtration (0.3 bar) through 0.4- $\mu\text{m}$  polycarbonate membranes (Osmonics). Clean sampling and handling techniques were used at every stage, and contamination control protocols were adhered to. For example, polyethylene gloves and a nylon coat were worn at all times; multistage cleaning procedures were used for LDPE bottles, Teflon vials, and filtration equipment; and sample handling and analysis—as well as the dispensing of ultrapure water (Milli-Q Element)—were carried out inside class 100 clean air cabinets (Bassaire).

*Determination of total dissolved and particulate metals*—Total metal concentrations in the dissolved and particulate phase were determined by competitive ligand equilibration–anodic stripping voltammetry (CLE-ASV) for Cu, by anodic stripping voltammetry (ASV) for Zn, and by cathodic stripping voltammetry (CSV) for Mn (Muller et al. 2003). The voltammetric system consisted of a Metrohm 693 VA Processor and a Metrohm 694 VA Stand with a glassy carbon electrode, which were coupled to an IBM ThinkPad 380XD portable computer. The reference electrode was Ag/AgCl, KCl (3 mol L<sup>-1</sup>), and the counter electrode was a platinum rod. Dissolved metals were determined after the ultraviolet digestion of acidified samples in silica tubes and adjustment of the pH prior to voltammetric analysis (Muller et al. 2003). Particulate metals were determined after the digestion of SPM collected on filters according to “Method A” described by Brüggemann and Kuss (1999); in this method, aqua regia was used to release the total trace metal content from the SPM, and the digestion was performed in polytetrafluoroethylene vessels (Bohlender GmbH) under pressure. The analytical precision of the measurements and their limit of detection are shown in Table 2. These values include the variability introduced by sample handling and, where appropriate, filter cleaning, rinsing, and weighing, but not that introduced by sampling. The accuracy of each of the analytical methods used for dissolved metal determination was

Table 2. Mean values of precision and detection limit for particulate metal content,  $[\text{M}_{\text{part}}]$ :SPM, dissolved metal concentration,  $[\text{M}_{\text{diss}}]$ , and titration parameters,  $C_{L,i}$  and  $K'_i$ .

Element	Property	Relative precision at the 90% probability level (%)	Detection limit at the 90% confidence level (nmol L <sup>-1</sup> )
Copper	$[\text{Cu}_{\text{part}}]$ :SPM	23	
	$[\text{Cu}_{\text{diss}}]$	12	0.2
	$C_{L,1}$	22	1.1
	$C_{L,2}$	15	1.1
	$C_{L,3}$	15	4.0
	$K'_1$	39	
	$K'_2$	30	
Zinc	$[\text{Zn}_{\text{part}}]$ :SPM	19	
	$[\text{Zn}_{\text{diss}}]$	11	0.4
	$C_{L,1}$	14	4.0
	$K'_1$	25	
	$K'_2$	27	
Manganese	$[\text{Mn}_{\text{part}}]$ :SPM	18	
	$[\text{Mn}_{\text{diss}}]$	11	2.0
	$C_{L,1}$	08	2.5
	$K'_1$	22	

verified by analyzing a nearshore seawater reference material (CASS-3, National Research Council of Canada) three times and checking the measured values ( $[\text{Cu}_{\text{diss}}] = 7.9 \pm 1.0$  nmol L<sup>-1</sup>;  $[\text{Zn}_{\text{diss}}] = 15.9 \pm 2.0$  nmol L<sup>-1</sup>; and  $[\text{Mn}_{\text{diss}}] = 38.6 \pm 4.2$  nmol L<sup>-1</sup>) against the certified ones ( $[\text{Cu}_{\text{diss}}] = 8.1 \pm 1.0$  nmol L<sup>-1</sup>;  $[\text{Zn}_{\text{diss}}] = 19.0 \pm 3.8$  nmol L<sup>-1</sup>; and  $[\text{Mn}_{\text{diss}}] = 45.7 \pm 6.5$  nmol L<sup>-1</sup>).

*Chemical speciation measurements*—Four different titrations were carried out on each sample. The first was a titration of the total Cu pool present in the sample with a well-characterized added ligand, ethylenediamine (EN), forming Cu complexes that are reversibly reduced and that thus control the measured peak current in the ASV method (Scarano et al. 1992; Muller et al. 2001). In this procedure, each sample filtrate was divided into 12 aliquots that were spiked with different concentrations of EN to produce a titration with constant increments of log  $[\text{EN}_T]$  (with  $[\text{EN}_T]$  expressed in nmol L<sup>-1</sup>) between -7.3 and -2.3. It allowed us to determine the concentrations ( $C_{L,1}$  and  $C_{L,2}$ ) and conditional stability constants ( $K'_1$  and  $K'_2$ ) of natural ligands forming strong complexes with Cu. The second titration was that of the excess complexing ligands present in the sample with incremental additions of Cu(II) ions to cover the range 0–800 nmol L<sup>-1</sup>. It allowed us to characterize ( $C_{L,3}$ ,  $K'_3$ ) the weaker, mostly unoccupied Cu-binding sites. In both titration procedures, the stripping peak current was recorded after the sample had been exchanged for a synthetic solution containing  $1.0 \times 10^{-2}$  mol L<sup>-1</sup> EN and  $0.5 \times 10^{-2}$  mol L<sup>-1</sup> HCl (pH 8.4). The third titration was with Zn(II) ions; the methodology and instrument settings were identical to those described by Muller et al. (2003). The fourth titration was a titration with Mn(II) ions monitored by CSV according to the method of Roitz and Bruland (1997).

The “labile” pool of each metal refers to those species

that contributed to the voltammetric signal to the same extent as the free metal ion. The deposition potentials chosen were designed to ensure that strong natural organic complexes would be kinetically inert (nonlabile). For each Zn and Mn, there was generally good agreement ( $r^2 \geq 0.80$ ,  $n = 37$ ) between the labile metal concentration measured directly and that calculated from total metal determination (previous section) and estimated complexation parameters (next section). On the other hand,  $[\text{Cu}_{\text{labile}}]$  values were systematically below the detection limit. Consequently, only the calculated labile metal concentrations have been listed.

**Speciation calculations**—The Cu complexation parameters ( $C_{L_i}$ ,  $K'_i$ ) were obtained by the nonlinear optimization of the two titration data sets using a Langmuir adsorption isotherm (Ružić 1982) to describe the extent of Cu binding. The EN titration curve systematically showed two inflexion points, thus indicating the presence of two high-affinity ligands. As a starting point, therefore, the portion of that curve starting at the base of the first wave rise was fitted to a two-ligand binding model according to

$$\frac{[\text{CuL}_1] + [\text{CuL}_2]}{[\text{Cu}^{2+}]} = \alpha_{\text{CuEN}} + \frac{C_{L1}}{[\text{Cu}^{2+}] + (1/K'_1)} + \frac{C_{L2}}{[\text{Cu}^{2+}] + (1/K'_2)} \quad (1)$$

Since the Cu-EN complexes contribute to the pool of labile Cu species,  $[\text{Cu}^{2+}]$  may be calculated at each concentration of added EN ( $[\text{EN}_T]$ ) according to

$$[\text{Cu}^{2+}] = \frac{[\text{Cu}_{\text{labile}}]}{1 + \alpha_{\text{inorg}} + \alpha_{\text{CuEN}}} \quad (2)$$

where  $\alpha_{\text{inorg}}$  is the coefficient representing the extent of inorganic complexation of Cu, and  $\alpha_{\text{CuEN}}$  is that representing the extent of complexation of Cu with EN. The value of  $\alpha_{\text{inorg}}$  was calculated from estimates of the free-ion molarities of  $\text{Cl}^-$ ,  $\text{OH}^-$ ,  $\text{HCO}_3^-$ ,  $\text{CO}_3^{2-}$ , and  $\text{SO}_4^{2-}$  and the corresponding stability constants obtained from the MINEQ+ thermodynamic database (Schecher and McAvoy 1998). Inorganic free-ion molarities were obtained from measurements of S,  $\text{pH}_{\text{SWS}}$ , and Alk and from the ion-pairing model of Kester (1986). The value of  $\alpha_{\text{CuEN}}$  was calculated from the relationship

$$\alpha_{\text{CuEN}} = K_{\text{CuEN}} \frac{[\text{EN}']}{\alpha_{\text{EN}}} + \beta_{\text{Cu(EN)}_2} \left( \frac{[\text{EN}']}{\alpha_{\text{EN}}} \right)^2 \quad (3)$$

where  $K_{\text{CuEN}}$  and  $\beta_{\text{Cu(EN)}_2}$  are the overall conditional stability constants of the CuEN and Cu(EN)<sub>2</sub> complexes,  $[\text{EN}']$  is the concentration of EN not complexed by Cu, and  $\alpha_{\text{EN}}$  describes the degree of association of EN with the  $\text{H}^+$  and  $\text{Mg}^{2+}$  present in seawater.

$$\alpha_{\text{EN}} = \frac{[\text{EN}']}{[\text{EN}_{\text{free}}]} = K_{\text{HEN}}[\text{H}^+] + \beta_{\text{H}_2\text{EN}}[\text{H}^+]^2 + K_{\text{MgEN}}[\text{Mg}^{2+}] \quad (4)$$

A first estimate of the parameters  $C_{L1}$ ,  $C_{L2}$ ,  $K'_1$ , and  $K'_2$  was obtained by the nonlinear regression analysis of Eq. 1, using

the Marquardt–Levenberg algorithm (SigmaStat 2.0, SPSS Science) to find the “best fit” between the equation and the EN titration data above  $[\text{EN}_T] \sim 10^{-6}$  M. A first estimate of the parameters  $C_{L3}$  and  $K'_3$  was obtained by the nonlinear fitting of the Cu titration data according to Eq. 5.

$$\frac{[\text{Cu}_T] - [\text{Cu}^{2+}]}{[\text{Cu}^{2+}]} = \alpha_{\text{inorg}} + \sum_{i=1}^3 \frac{C_{L_i}}{[\text{Cu}^{2+}] + (1/K'_i)} \quad (5)$$

This ( $C_{L3}$ ,  $K'_3$ ) estimate was then plugged back into the complete form of Eq. 1 describing the full EN titration curve, namely

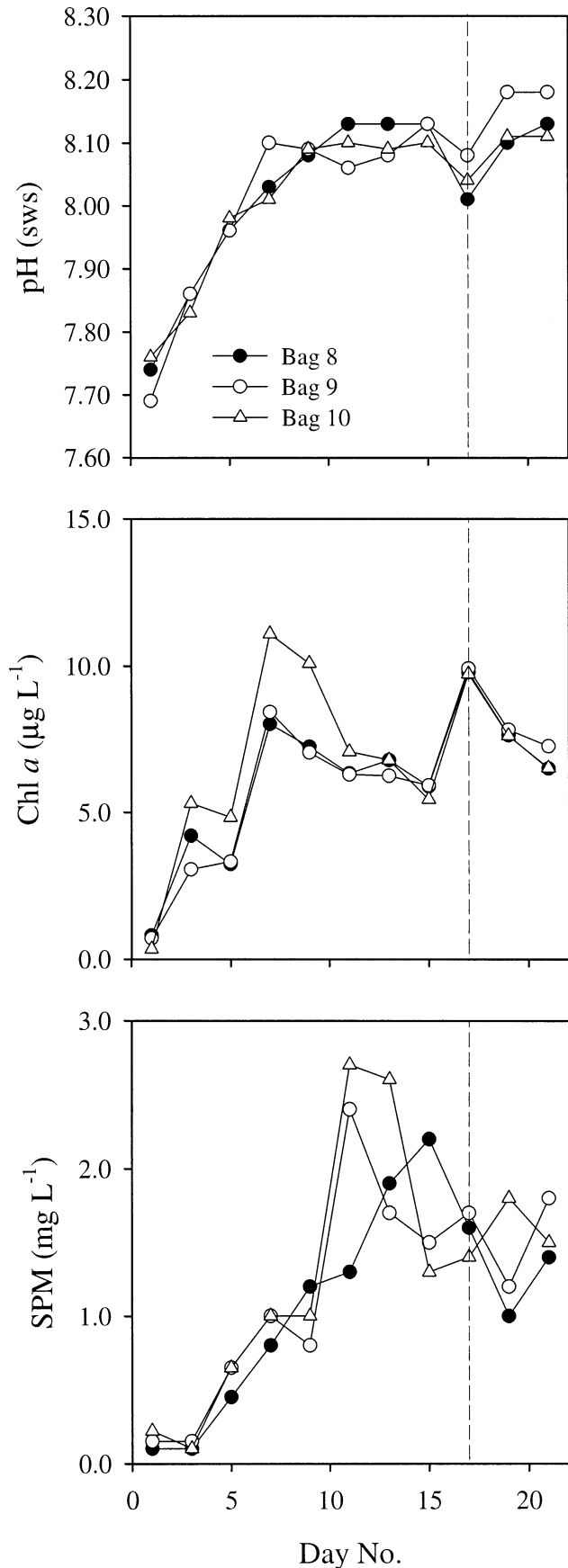
$$\frac{[\text{CuL}_1] + [\text{CuL}_2] + [\text{CuL}_3]}{[\text{Cu}^{2+}]} = \alpha_{\text{inorg}} + \alpha_{\text{CuEN}} + \sum_{i=1}^3 \frac{C_{L_i}}{[\text{Cu}^{2+}] + (1/K'_i)} \quad (6)$$

and new estimates of  $C_{L1}$ ,  $C_{L2}$ ,  $K'_1$ , and  $K'_2$  were obtained by the nonlinear regression analysis of Eq. 6. The iterative process between the EN titration curve (evaluation of  $C_{L1}$ ,  $C_{L2}$ ,  $K'_1$ , and  $K'_2$ ) and the Cu titration curve (evaluation of  $C_{L3}$  and  $K'_3$ ) was performed three times; further iterations did not change the parameter values. For Zn and Mn, only one titration with the metal of interest was conducted, and the curve could be accurately described by a one-metal–one-ligand Langmuir isotherm (same form as Eq. 5, with  $i = 1$ ). The parameters  $C_{L1}$  and  $K'_1$  were thus obtained directly by the nonlinear fitting of the titration curve. Three ligands ( $i = 1, 2,$  and  $3$ ) for Cu and one ligand ( $i = 1$ ) for Zn or Mn were required to fit the titration curves. The last step was to calculate the portions ( $\text{ML}_1$ ,  $\text{ML}_2$ , etc.) of the metal that were bound to these ligands and the portion ( $\text{M}_{\text{labile}}$ ) that was soluble and not complexed by any organic ligand. This was done using the chemical equilibrium modeling software MINEQ+ (version 4.0; Schecher and McAvoy 1998).

The 90% confidence intervals for the metal complexation parameters were provided as part of the nonlinear regression analyses. Average errors in  $C_{L_i}$  and  $K'_i$  are presented in Table 2, together with errors in dissolved and particulate metal concentrations provided by the linear regression of standard addition curves.

## Results

Apart from the fact that the peak values in Chl *a*, SPM (Fig. 2), algal populations (Fig. 3), and Cu-binding ligand concentrations (Fig. 4) were generally 10–30% higher in bag 10 than the corresponding peak values in bag 8 or 9, neither these properties nor the Zn or Mn speciation parameters were significantly affected by the different N:P ratios. Therefore, bags 8–10 can be seen as three replicates from “one” bag. In the morning hours of day 17, there was 76 mm of rain. This precipitation event came after a 4-week period of nearly uninterrupted dry and sunny weather (cumulative precipitation during the preceding 4 weeks = 34 mm). It was accompanied by significant increases in Cu (Fig. 4), Zn (Fig. 5), and Mn concentrations (Fig. 6)—but also dissolved inorganic nitrogen (Table 1)—in the bags and in the surface waters of the fjord. Finally, a striking feature was



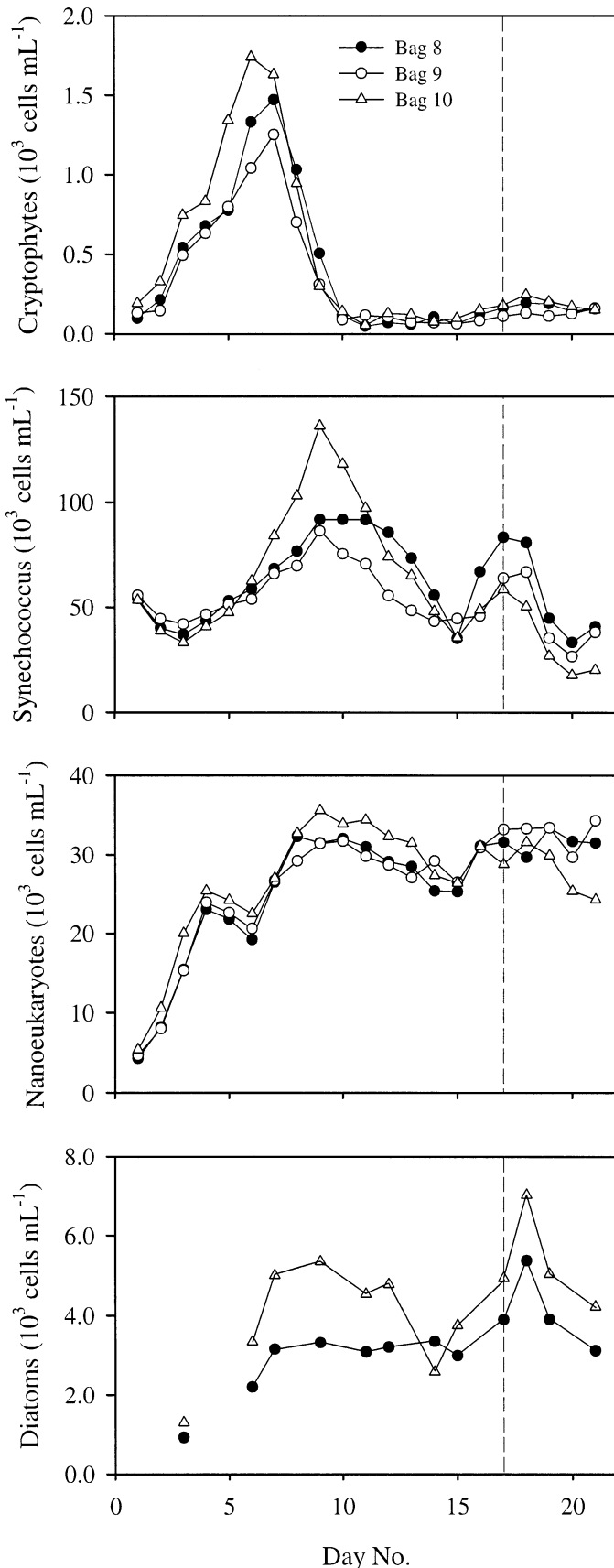
the lack of correspondence in the timing of the major changes observed in the speciation of the three metals. For example,  $[\text{Cu}_{\text{labile}}]$  began to decrease sharply on day 1,  $[\text{Mn}_{\text{labile}}]$  began to decrease on day 3, and  $[\text{Zn}_{\text{labile}}]$  began to decrease on day 5. This lack of covariance between the fates of labile Cu, Mn, and Zn suggests that they were controlled by different processes.

*Nutritional conditions and indicators of photosynthetic activity*—A steady increase in both pH and chlorophyll took place from days 1 to 9, followed by a plateau reached between days 10 and 16 (Fig. 2). The rain event (day 17) appears to have temporarily stimulated phytoplankton production—as shown by the second peak in chlorophyll (Fig. 2). It is worth mentioning that, between days 10 and 16, chlorophyll values developed to markedly higher values in mesocosms where N was added in excess of the Redfield ratio (bags 6 and 7; data not shown). Moreover, the rain event did not produce a peak in chlorophyll in the mesocosm that was receiving the largest daily doses of N, i.e., bag 6. These two observations suggest that bags 8–10 were in fact N limited between days 10 and 16. On day 17, pH showed a minimum due to the addition of rain to the bags, but it recovered quickly as a result of ongoing photosynthetic activity. Inorganic N and P concentrations in bags 8–10 ranged between 0.2 and 0.5 and 0.04 and 0.17  $\mu\text{mol L}^{-1}$ , respectively (Table 1). From day 9 onward, inorganic N concentrations appeared to be the main variable limiting phytoplankton growth in bags 8–10. These concentrations increased slightly—while phosphate concentrations were approximately halved—between days 15 and 17, i.e., during the full duration of the rain event. Silicate concentrations in each of the bags peaked at around 6–7  $\mu\text{mol L}^{-1}$  on day 7 and then decreased exponentially to reach final values of 1.7, 0.9, and 0.4  $\mu\text{mol L}^{-1}$  in bags 8, 9, and 10, respectively.

*Phytoplankton bloom dynamics*—The population of cyanobacteria *Synechococcus* sp. peaked twice during the experimental period and numerically dominated the algal community until day 18, 1 d after the rain event (Table 3; Fig. 3). Nanoeukaryotes showed an increase in cell density between days 1 and 8, followed by relatively small fluctuations. Diatom abundance (determined by light microscopy, hence the different sampling resolution seen in Fig. 3) also increased up to day 7 or 8 and then leveled off. Cryptophytes reached their maximum cell density on days 7–8 and then crashed for 3 d (Fig. 3). All algal groups showed an increase from days 15 to 17. Since physical parameters (temperature,

←

Fig. 2. Time series showing the development of pH, Chl *a*, and suspended particulate matter in each of the bags. All bags received the same daily additions of inorganic nutrients (N, P, and Si) until day 7 inclusive. After day 7, daily phosphate additions were maintained at 0.05  $\mu\text{mol L}^{-1}$  in bag 8 but were stepped up to 0.1  $\mu\text{mol L}^{-1}$  and 0.2  $\mu\text{mol L}^{-1}$  in bags 9 and 10, respectively. Day 17 is identified by a vertical line as the corresponding data points refer to samples collected only 3 h after the end of the 8-h-long rain event.



light intensity, mixing, pH, and macronutrient concentrations) were relatively constant around day 15, one possible explanation for the concomitant increase in the abundance of cryptophytes, *Synechococcus*, nanoeukaryotes, and diatoms could have been a reduction in grazing pressure (not measured). The rain event, on day 17, seemed to enhance the second diatom bloom.

**Copper**—Total and dissolved Cu concentrations were nearly indistinguishable from each other, as the particulate phase accounted for only 0.2 (days 1–3) to 0.8 (days 17–21)  $\text{nmol L}^{-1}$  Cu. On the other hand, the Cu content of SPM showed a clear decrease (with the exception of two anomalous data points shown in parentheses in Fig. 4) from day 1 ( $\sim 60 \text{ mg kg}^{-1}$ ) to day 15 ( $\sim 20 \text{ mg kg}^{-1}$ ) and a sudden increase back to levels around 30–40  $\text{mg kg}^{-1}$  on day 17 (rain event). Dissolved Cu concentrations also increased during the rain event but dropped down for 2 d to the levels observed before the event. The lowest concentrations of labile Cu were observed at the end of the exponential growth phase of diatoms (day 5), as well as during the days following the rain event (days 19–21). At these times, the total concentration of strongly binding ligands,  $C_{L1} + C_{L2}$ , equaled or exceeded the concentration of dissolved Cu, as shown in Table 4. In view of the binding strength of these two ligands, it is easy to understand why they dominated Cu speciation and why their relative contributions to Cu speciation showed opposite variations (Fig. 7). The concentration of weakly binding ligands,  $C_{L3}$ , increased almost linearly from 25 to 40  $\text{nmol L}^{-1}$  on day 1 to 200–270  $\text{nmol L}^{-1}$  on day 11 and then leveled off at around 150–220  $\text{nmol L}^{-1}$  for the rest of the experiment. Although  $L_3$  bound only 0.3–5% of dissolved Cu most of the time, it did play an important role on day 17 (16–19% of dissolved Cu present as  $\text{CuL}_3$ ) by binding most of the excess Cu deposited by rain and thus buffering the free Cu ion concentration (Fig. 7). In addition, it is worth noting that, between days 1 and 11,  $C_{L3}$  was highly correlated to the so-called proteinlike DOM fluorescence (Fig. 8). This correlation ( $r^2 = 0.90$ ,  $n = 19$ ) was significantly higher than the next best correlation, which was that between  $C_{L3}$  and Chl *a* ( $r^2 = 0.75$ ,  $n = 16$ ). Proteinlike fluorescence properties (excitation maximum at 275 nm; emission maxima at 306 and 338 nm) have been frequently reported in productive marine waters (Yamashita and Tanoue 2003), algal blooms (Determann et al. 1994), sediment pore waters (Coble 1996), and cultures of marine bacteria and phytoplankton (Determann et al. 1998). These properties are nearly identical to those of two individual amino acids that have an aromatic ring, namely tyrosine (Ex = 275 nm; Em = 305 nm) and tryptophan (Ex = 275 nm; Em = 340 nm).

**Zinc**—Particulate Zn concentrations increased dramatically from 0.5  $\text{nmol L}^{-1}$  (day 1) to 12  $\text{nmol L}^{-1}$  (day 17). Some of this increase was accounted for by an increase in SPM,

Fig. 3. Cell densities of cryptophytes, *Synechococcus* sp., nanoeukaryotes, and diatoms, all expressed in  $10^3 \text{ cells mL}^{-1}$ . Vertical line indicates the day (day 17) of exceptional rainfall.

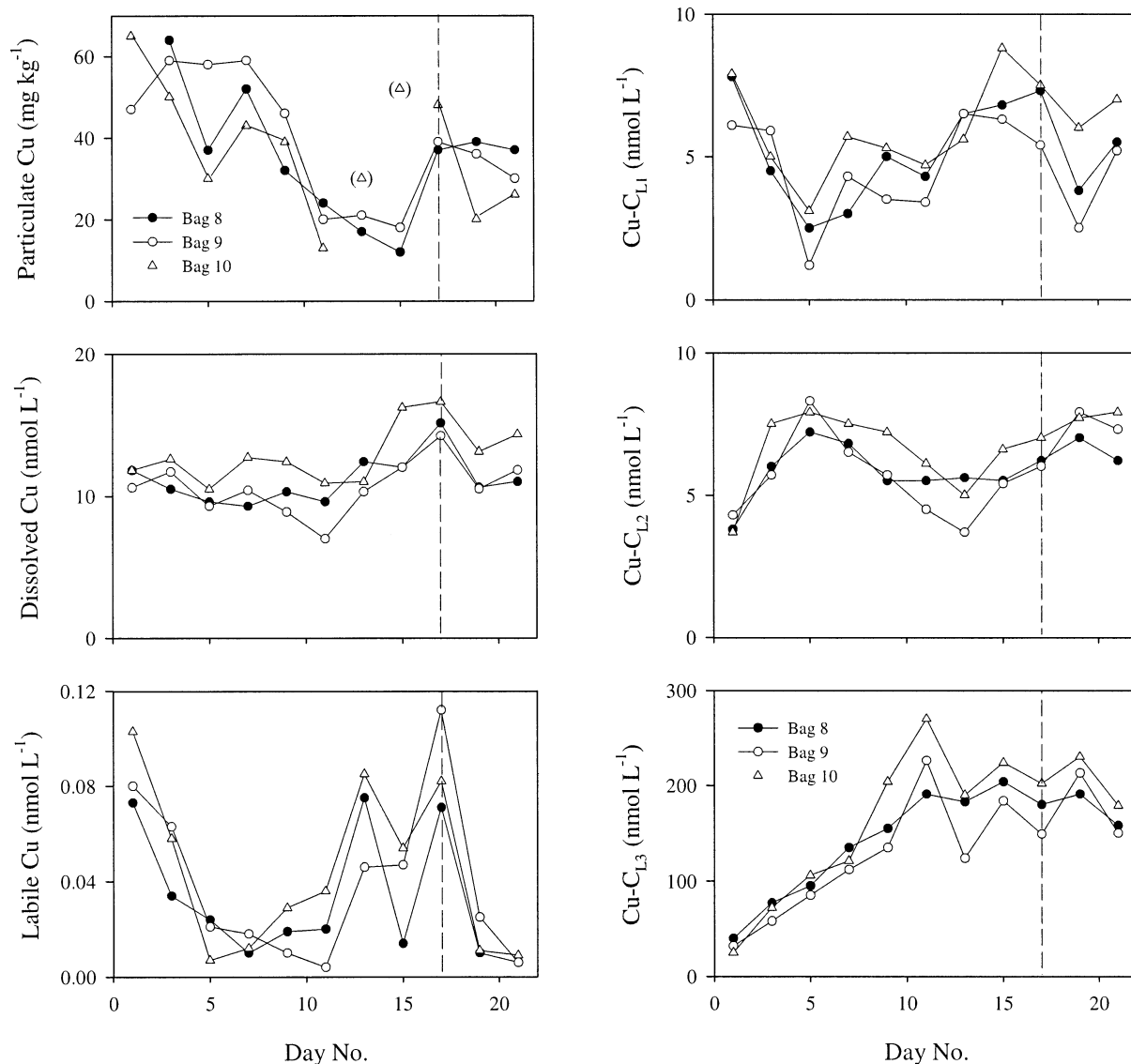


Fig. 4. Concentrations of particulate Cu (in the particulate phase), dissolved Cu, and labile Cu and Cu-binding ligands denoted L<sub>1</sub> through L<sub>3</sub> in order of decreasing binding strength.

and the rest was accounted for by an increase in the Zn content of the SPM from ~200 to ~500 mg kg<sup>-1</sup> (Fig. 5). During the same period, i.e., prior to the rain event, particulate and dissolved Zn concentrations varied in opposite directions, but the global magnitude of these changes was about the same (~12 nmol L<sup>-1</sup>). The highest concentrations of labile Zn were observed at the beginning of the experiment (days 1–5). After declining sharply between days 5 and 11, labile Zn concentrations remained uniformly low until the end of the experiment (Fig. 5). The decline in [Zn<sub>labile</sub>] was due to the combination of increasing Zn-binding ligands, C<sub>L1</sub>, concurrently with decreasing dissolved Zn concentrations, [Zn<sub>diss</sub>], which took place between days 7 and 11 (Fig. 5).

**Manganese**—Total and dissolved Mn variations generally followed each other. On day 17, however, total Mn concen-

trations (data not shown) rose by 14 nmol L<sup>-1</sup> above values observed 2 d before or after, whereas dissolved Mn concentrations (Fig. 6) rose by only 6 nmol L<sup>-1</sup>. The corresponding increase in particulate Mn concentrations was due to Mn enrichment of the particulate phase (Fig. 6), probably due to direct sorption of Mn dissolved in rainwater to the particulate phase in seawater, as the SPM itself clearly did not increase (Fig. 2). Labile Mn concentrations showed variations that were only weakly correlated with those in dissolved Mn (Fig. 6); the lowest [Mn<sub>labile</sub>] values were observed on days 7 and 9, and these coincided with the highest heterotrophic bacterial cell numbers (Fig. 9), as had been observed before in the Raunefjord (Muller et al. 2003). Labile Mn concentrations did not show such a tight inverse correlation with variations in cyanobacterial cell numbers, which were shifted by 1–2 d relative to variations in heterotrophic bacteria. In contrast to the seawater speciation of Cu and Zn, Mn spe-

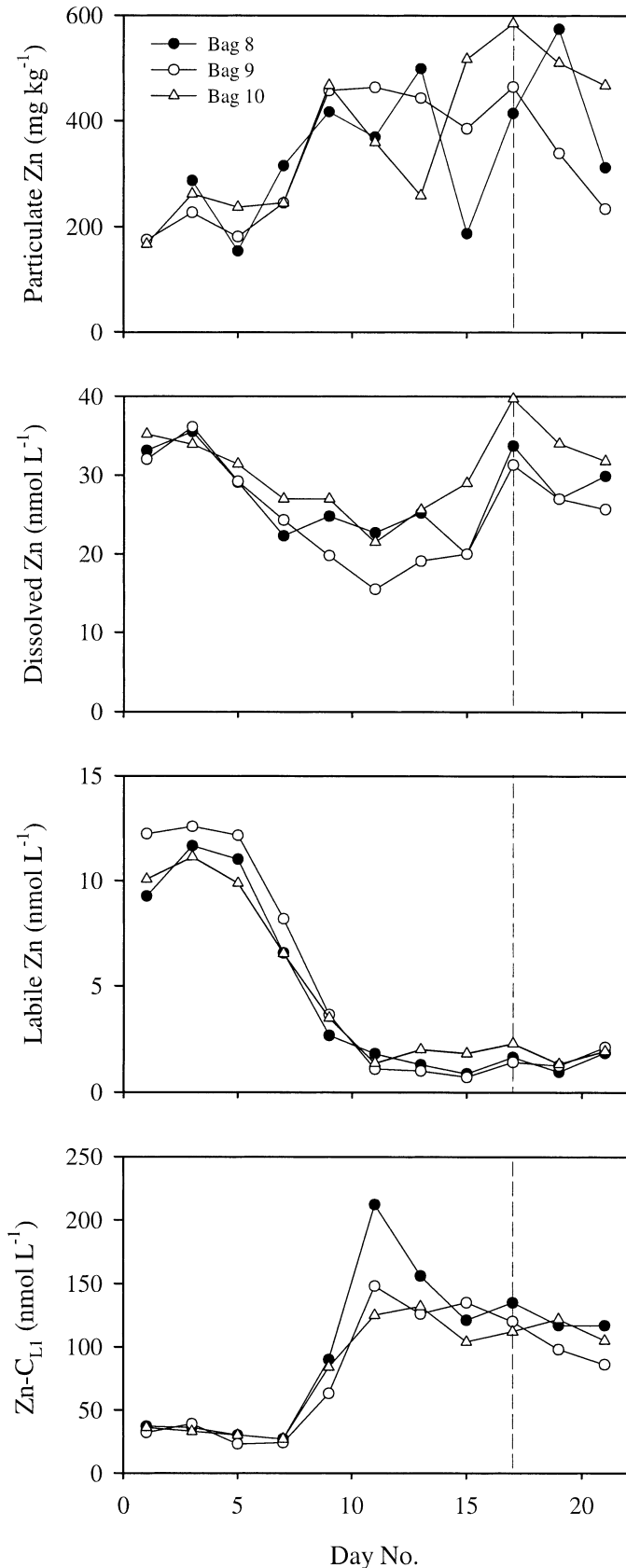


Fig. 5. Concentrations of particulate Zn (in the particulate phase), dissolved Zn, labile Zn, and Zn-binding ligands.

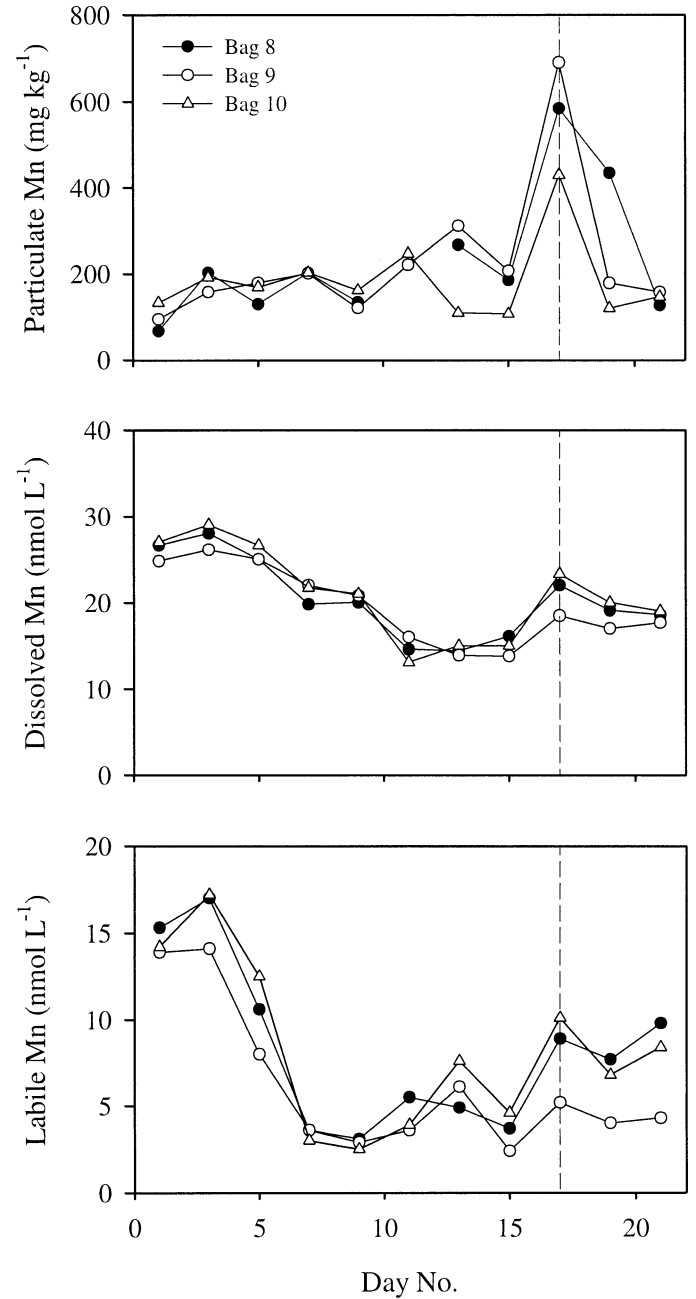


Fig. 6. Concentrations of particulate Mn (in the particulate phase), dissolved Mn, and labile Mn.

ciation is generally dominated by kinetically labile inorganic forms (Roitz and Bruland 1997). Organic complexation of Mn has only been reported once in a marine system characterized by high organic matter decomposition and low oxygen concentrations (Luther et al. 1994). It follows that, unlike the organic ligands that complexed Cu or Zn, the Mn-binding sites—as derived through modeling of our titration data—were unlikely to have existed as organic ligands. As we are unsure about their exact physical nature, we have neither shown nor discussed their temporal variations as we have for the Cu-binding or Zn-binding ligands.

Table 3. Auxilliary variables used to interpret the changes in metal speciation observed during the course of the mesocosm experiment. Chlorophyll, heterotrophic bacteria and algal groups were measured everyday but only measurements backed up by trace metal data (Tables 4-6) are shown. ND, not determined.

Day	S	pH <sub>sws</sub>	Alk (meq L <sup>-1</sup> )	Chl <i>a</i> (μg L <sup>-1</sup> )	Fluor-4 (nm <sup>-1</sup> )	SPM (mg L <sup>-1</sup> )	(10 <sup>3</sup> cells mL <sup>-1</sup> )			
							H-bact	Syne	Nano	Crypto
Bag 8, depth = 2 m										
1	28.3	7.74	2.104	0.80	0.064	0.10	1,560	54	4.3	0.10
3	28.3	7.86	2.078	4.20	0.197	0.10	1,680	37	15.4	0.54
5	28.3	7.96	2.070	3.23	0.258	0.45	2,840	53	21.8	0.77
7	28.1	8.03	2.033	8.01	0.285	0.80	5,530	68	26.5	1.47
9	28.2	8.08	2.014	7.23	0.398	1.20	5,750	92	31.5	0.50
11	28.4	8.13	2.027	6.32	0.405	1.30	5,130	91	31.0	0.05
13	28.5	8.13	2.021	6.77	0.320	1.90	2,820	73	28.5	0.06
15	28.6	8.13	2.021	5.88	0.400	2.20	3,350	35	25.3	0.06
17	28.0	8.01	1.980	9.79	ND	1.60	4,450	83	31.6	0.16
19	28.1	8.10	1.978	7.62	0.287	1.00	3,930	45	33.4	0.19
21	28.2	8.13	1.994	6.49	0.347	1.40	3,730	41	31.5	0.16
Bag 9, depth = 2 m										
1	28.4	7.69	2.099	0.70	0.029	0.15	1,620	56	4.7	0.13
3	28.6	7.86	2.088	3.05	0.115	0.15	1,570	42	15.3	0.49
5	28.5	7.96	2.096	3.32	0.170	0.65	2,800	51	22.6	0.79
7	28.5	8.10	2.060	8.42	0.308	1.00	5,440	66	26.7	1.25
9	28.5	8.09	2.038	7.03	0.418	0.80	5,670	86	31.4	0.31
11	28.6	8.06	2.020	6.28	0.359	2.40	4,430	70	29.8	0.11
13	28.7	8.08	2.026	6.24	0.285	1.70	2,970	48	27.1	0.07
15	28.9	8.13	2.033	5.91	0.348	1.50	3,390	45	26.5	0.06
17	28.4	8.08	1.995	9.91	ND	1.70	4,760	64	33.2	0.11
19	28.4	8.18	1.997	7.81	0.205	1.20	4,350	35	33.4	0.11
21	28.4	8.18	2.000	7.25	0.273	1.80	5,360	38	34.3	0.16
Bag 10, depth = 2 m										
1	28.5	7.76	2.106	0.34	0.032	0.22	1,860	53	5.4	0.19
3	28.6	7.83	2.091	5.30	0.165	0.10	1,950	33	20.0	0.74
5	28.6	7.98	2.079	4.83	0.248	0.65	3,800	48	24.2	1.34
7	28.6	8.01	2.049	11.09	0.353	1.00	7,060	84	27.0	1.63
9	28.5	8.09	2.026	10.09	0.446	1.00	7,100	136	35.6	0.30
11	28.6	8.10	2.027	7.06	0.445	2.70	3,510	97	34.4	0.05
13	28.8	8.09	2.014	6.78	0.402	2.60	3,240	65	31.5	0.12
15	28.9	8.10	2.023	5.44	0.502	1.30	4,160	36	26.4	0.10
17	28.4	8.04	1.984	9.73	ND	1.40	4,580	59	28.8	0.18
19	28.6	8.11	1.989	7.61	0.222	1.80	3,520	27	29.9	0.20
21	28.4	8.11	1.977	6.51	0.325	1.50	3,750	20	24.3	0.15
Raunefjord, depth = 6 m										
7	28.6	7.86	2.060	3.21	0.162	0.23	2,240	109	7.5	0.32
11	28.8	7.85	2.052	2.09	0.216	0.47	3,460	205	2.1	0.33
15	29.0	7.92	2.059	3.21	0.352	1.50	3,660	253	4.7	0.31
19	28.6	8.00	2.016	3.11	0.345	0.60	2,790	148	11.3	0.67

## Discussion

*Intervention of the microbial community in regulating the availability of Mn and Cu*—Although Mn is required by all photosynthetic organisms, it was the inverse correspondence between labile Mn concentration and heterotrophic bacterial abundance that provided the most striking covariation, as noted above. It is presented in Fig. 9 and is consistent with a dynamic and reversible redox cycle whereby Mn<sup>2+</sup> is oxidized by microbial processes while colloidal Mn-oxides are simultaneously reduced back to Mn<sup>2+</sup>. The trend observed at any point in time thus reflects the dynamic balance be-

tween these two processes. Heldal et al. (1996) have reported the ubiquitous occurrence in these fjordic waters of a relatively abundant group of bacteria that sequester large amounts of Fe and Mn on extracellular appendages. On the basis of the total counts and metal contents of Mn-Fe bacterial cells recorded in the Raunefjord in June 1993 (Heldal et al. 1996), we estimate that this group of bacteria could potentially have trapped 2.7–7.5 nmol L<sup>-1</sup> of Mn. This estimation is based on the bacterial cell counts and mean cellular Mn quota reported by Heldal et al. (1996), namely 5.5–15.0 × 10<sup>3</sup> mL<sup>-1</sup> and 25 fg Mn cell<sup>-1</sup>. Had they bloomed in the bags, this group of bacteria could thus have accounted

Table 4. Dissolved, labile, and free Cu concentrations, Cu-binding ligand concentrations, and related conditional stability constants measured during the course of the mesocosm experiment.

Day	(nmol L <sup>-1</sup> )			(nmol L <sup>-1</sup> )			log K <sub>1</sub>	C <sub>L2</sub> (nmol L <sup>-1</sup> )	log K <sub>2</sub>	C <sub>L3</sub> (nmol L <sup>-1</sup> )	log K <sub>3</sub>
	[Cu <sub>dis</sub> ]	[Cu <sub>labile</sub> ]	α-inorg	[Cu <sup>2+</sup> ]	C <sub>L1</sub>	log K <sub>1</sub>					
Bag 8, depth = 2 m											
1	11.8	0.073	8.0	0.0091	7.8	15.40	3.8	13.28	40	8.61	
3	10.5	0.034	10.3	0.0033	4.5	15.65	6.0	13.07	77	8.66	
5	9.6	0.024	12.3	0.0019	2.5	15.48	7.2	13.30	95	8.48	
7	9.3	0.010	13.5	0.0008	3.0	15.42	6.8	13.17	135	8.65	
9	10.3	0.019	14.5	0.0013	5.0	15.39	5.5	13.17	155	8.45	
11	9.6	0.020	15.6	0.0013	4.3	15.24	5.5	13.20	191	8.18	
13	12.4	0.075	15.7	0.0048	6.5	15.50	5.6	13.35	183	8.50	
15	12.0	0.014	15.7	0.0009	6.8	15.81	5.5	13.12	204	8.83	
17	15.1	0.071	13.1	0.0054	7.3	15.48	6.2	13.09	180	9.22	
19	10.6	0.019	14.8	0.0013	3.8	15.44	7.0	13.30	143	9.39	
21	11.0	0.006	15.5	0.0004	5.5	15.33	6.2	13.21	158	9.27	
Bag 9, depth = 2 m											
1	10.6	0.080	7.1	0.0113	6.1	15.46	4.3	13.20	32	8.60	
3	11.7	0.063	10.4	0.0060	5.9	15.85	5.7	13.10	58	8.51	
5	9.3	0.021	12.4	0.0017	1.2	15.56	8.3	13.27	85	8.36	
7	10.4	0.018	15.1	0.0012	4.3	15.50	6.5	13.00	112	8.77	
9	8.9	0.010	14.9	0.0007	3.5	15.90	5.7	13.34	135	8.38	
11	7.0	0.004	14.3	0.0003	3.4	15.52	4.5	13.10	226	8.22	
13	10.3	0.046	14.8	0.0031	6.5	15.74	3.7	13.24	124	8.50	
15	12.0	0.047	15.9	0.0026	6.3	15.71	5.4	13.16	184	8.93	
17	14.2	0.112	14.6	0.0078	5.4	15.68	6.0	13.36	149	9.38	
19	10.5	0.033	16.5	0.0020	2.5	15.69	7.9	13.01	133	9.23	
21	11.8	0.006	16.5	0.0004	5.2	15.53	7.3	13.30	150	9.30	
Bag 10, depth = 2 m											
1	11.8	0.103	8.5	0.0122	7.9	15.60	3.7	13.15	25	8.59	
3	12.6	0.058	9.9	0.0059	5.0	15.65	7.5	13.11	72	8.51	
5	10.5	0.007	12.8	0.0006	3.1	15.84	7.9	13.40	106	8.59	
7	12.7	0.012	13.4	0.0009	5.7	15.47	7.5	13.14	121	8.55	
9	12.4	0.029	14.9	0.0019	5.3	15.69	7.2	13.19	204	8.42	
11	10.9	0.036	15.1	0.0024	4.7	15.48	6.1	13.20	270	8.52	
13	11.0	0.085	15.0	0.0056	5.6	15.86	5.0	12.98	190	8.58	
15	16.2	0.054	15.3	0.0036	8.8	15.96	6.6	13.25	224	9.03	
17	16.6	0.082	13.8	0.0060	7.5	15.52	7.0	12.91	202	9.26	
19	13.1	0.012	15.3	0.0008	6.0	15.60	7.7	13.03	150	9.27	
21	14.3	0.009	15.2	0.0006	7.0	15.80	7.9	13.22	179	9.20	
Raunefjord, depth = 5 m											
7	10.9	0.008	11.5	0.0007	2.9	15.32	8.8	13.14	75	9.00	
11	11.9	0.029	11.3	0.0025	4.9	15.65	7.1	12.95	103	8.82	
15	13.0	0.008	12.8	0.0007	8.1	15.76	5.3	13.19	140	8.77	
19	15.5	0.006	13.7	0.0004	10.3	15.43	5.9	13.20	148	9.13	

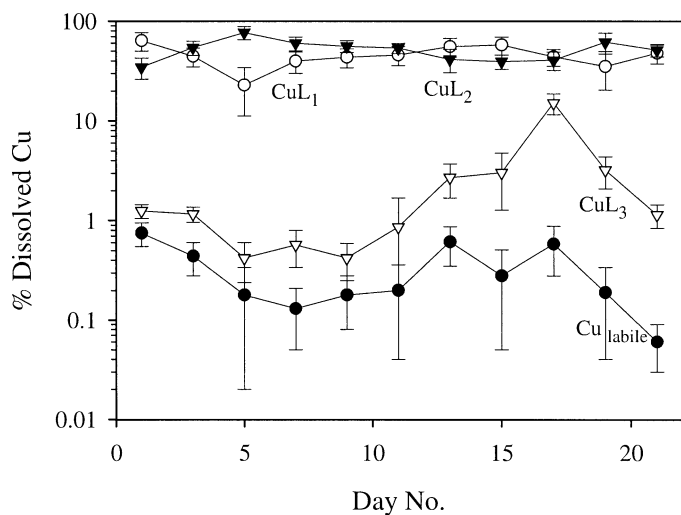


Fig. 7. Temporal changes in the fractional composition of dissolved Cu. Percent values are averages between the three bags, and errors are at the 90% confidence level. Note that the ordinate is logarithmic.

for the magnitude of the  $[\text{Mn}_{\text{labile}}]$  decrease ( $\sim 5 \text{ nmol L}^{-1}$ ) observed between days 3 and 7 (Fig. 9). During daytime hours, sunlight must have decreased the rate of bacterially mediated Mn-oxide formation while also increasing the rate of the reductive dissolution of the Mn oxides (Sunda and Huntsman 1994). The latter process would have been assisted by the continuous presence in these waters of humic substances, which were identified from the peak position of their fluorophores ( $\text{Ex} = 350 \text{ nm}$ ;  $\text{Em} = 445 \text{ nm}$ ); these peaks (Stedmon and Markager pers. comm.) had the same position when compared with fluorophores previously reported for marine humiclike substances (Coble 1996; Yamashita and Tanoue 2003). Interestingly, there is evidence from the recent literature (Parlanti et al. 2000; Rochelle-Newall and Fisher 2002; Stedmon and Markager pers. comm.) to the effect that marine humiclike fluorophores are produced during the microbial degradation of organic matter. Several of the humiclike fluorophores identified during our study were found to be microbially generated during sample incubation experiments (Stedmon and Markager pers. comm.), which supports the conclusion that they were derived from microbial activity in the bags and fjord.

Organic complexation of Cu with the ligands  $L_1$ ,  $L_2$ , and  $L_3$  reduced the concentration of labile Cu,  $[\text{Cu}_{\text{labile}}]$ , to values between 0.004 and 0.112  $\text{nmol L}^{-1}$  during the course of the experiment (Table 4). The  $\text{CuL}_1$  and  $\text{CuL}_2$  complexes comprised 80–99.8% of the dissolved Cu species, most of the remainder being present as  $\text{CuL}_3$  (Fig. 7). The sum of the concentrations of the two strong ligands,  $C_{L1} + C_{L2}$ , nearly matched the dissolved Cu concentration throughout (Fig. 8). The dominance of seawater Cu speciation by strong organic ligands at concentrations near dissolved Cu levels has been widely reported in both oceanic and coastal surface waters (Moffett et al. 1997; Croot et al. 2000; Croot 2003). It has been proposed that these ligands have a biological origin and that their observed covariation with dissolved Cu is part of a mechanism used by cyanobacteria (Moffett et al. 1997)

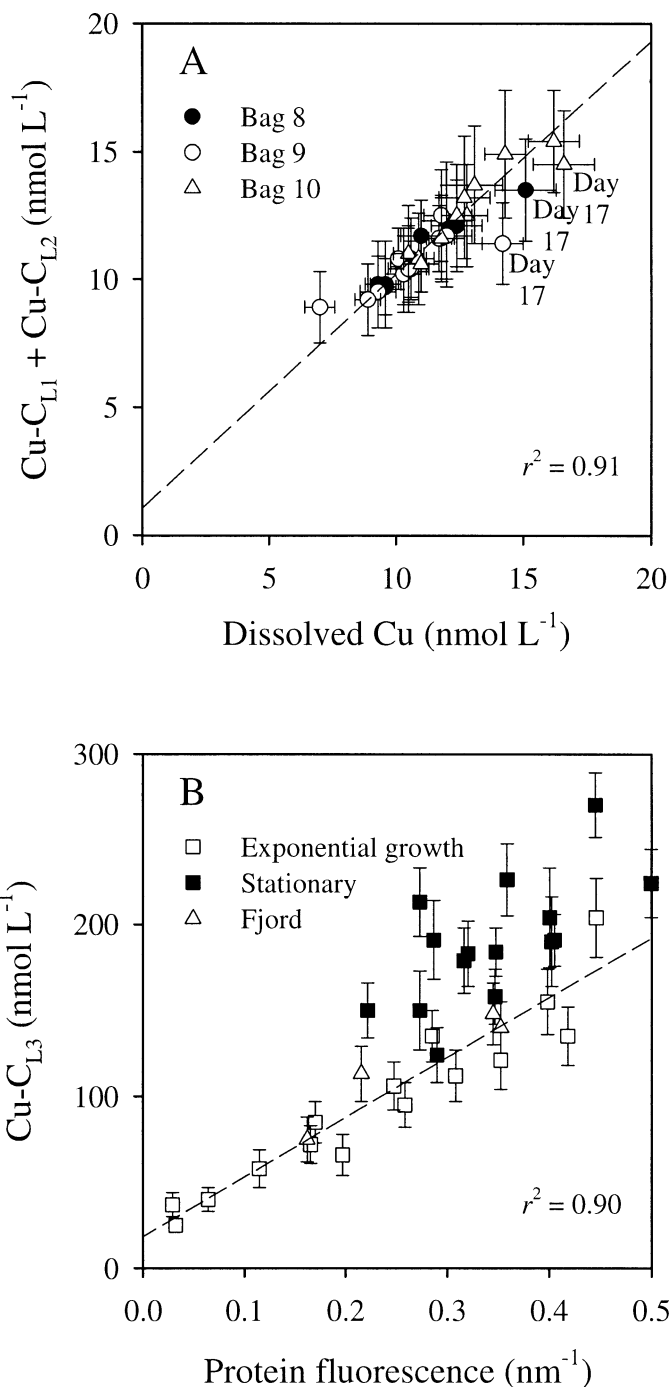


Fig. 8. (A) Total concentration of strong Cu-binding ligands plotted against the dissolved Cu concentration; 90% confidence limits for slope and intercept are  $0.91 \pm 0.07$  and  $1.1 \pm 0.7$ , respectively. (B) Concentration of weak Cu-binding ligands plotted against the proteinlike fluorescence that was derived by the method of Stedmon et al. (2003) and expressed in Raman units (R.U.,  $\text{nm}^{-1}$ ); only data points from the exponential growth phase are included in the regression; 90% CL for slope and intercept are  $348 \pm 55$  and  $18 \pm 14$ , respectively.

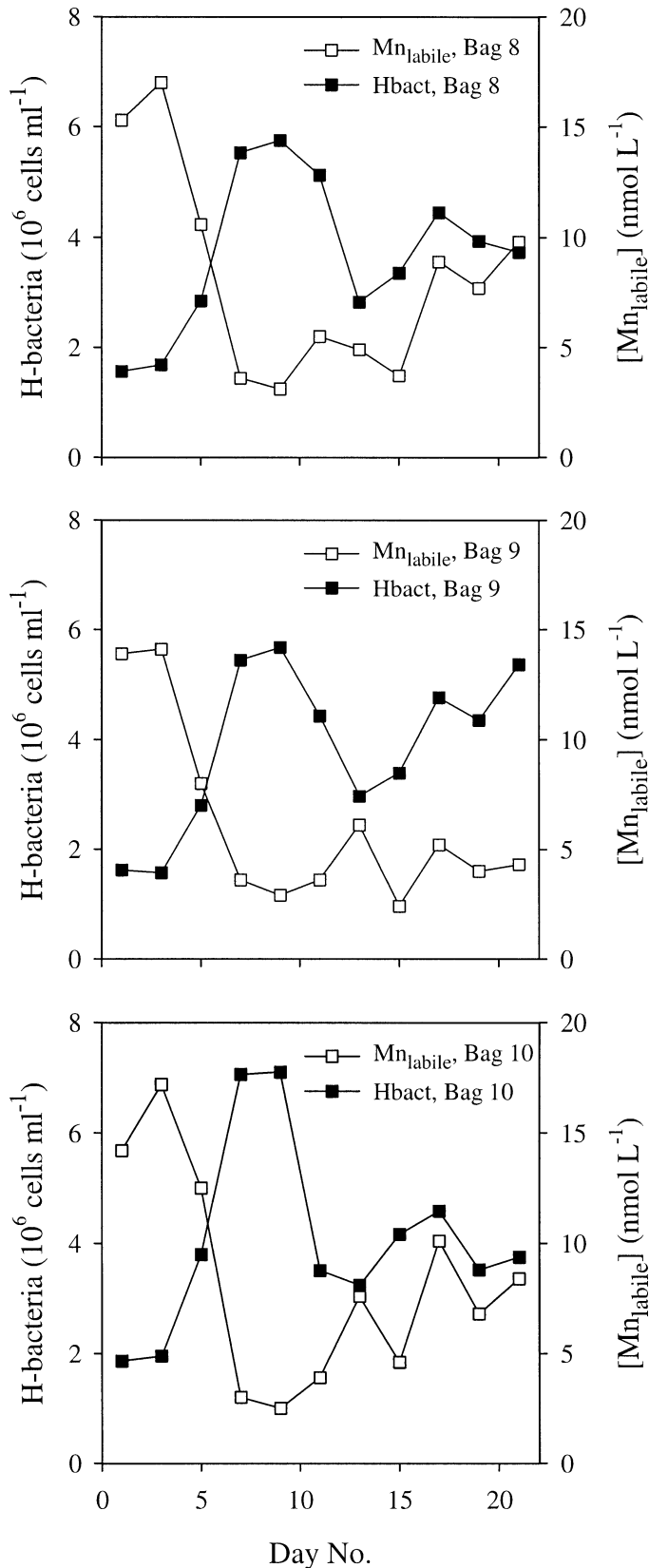


Fig. 9. Comparison of the variations in bacterial numbers and labile Mn concentrations in each bag.

and eukaryotic phytoplankton (Croot et al. 2000) to detoxify Cu. Prokaryotes, such as the cyanobacterium *Synechococcus* sp., are known to be much more susceptible to Cu toxicity than eukaryotes. As *Synechococcus* sp. numerically dominated the algal community in our experiment (Fig. 3), except during the last 3 d (days 19–21), it might have been a source of the  $L_1$  and  $L_2$  ligands. In the fjord as in the bags, the covariation of  $C_{L1} + C_{L2}$  with  $[Cu_{diss}]$ , together with the presence of a large excess of  $L_3$  ligands at times when  $[Cu_{diss}]$  exceeded  $C_{L1} + C_{L2}$ , maintained  $[Cu_{labile}]$  in the range of 0.004–0.112 nmol L<sup>-1</sup> (pCu = 11.2–12.4), i.e., below the toxicity threshold for *Synechococcus* sp. (Moffett and Brand 1996). These values were significantly lower (higher pCu) than those measured during the spring 2000 experiment (pCu = 10.0–11.1; Muller et al. 2003) when *Synechococcus* sp. were also less abundant. In addition,  $L_2$  ligands had conditional stability constants ( $12.9 < \log K'_2 < 13.4$ ) that matched those measured in laboratory cultures of *Synechococcus* (Croot et al. 2000) as well as in coastal (Moffett et al. 1997) and fjordic environments (Croot 2003; Muller et al. 2003) during times of significant *Synechococcus* abundance. However, one cannot totally exclude the possibility that  $L_2$  was synthesized by eukaryotic phytoplankton (compare the time series of diatoms and  $C_{L2}$  in Figs. 3, 4, respectively) for a purpose other than detoxification, e.g., for nitrogen storage and assimilation. Such a biochemical role has been recently proposed by Dupont et al. (2004) for novel Cu-binding, N-rich thiols produced in cultures of *Emiliania huxleyi*. Interestingly, the relative importance of our  $L_2$  ligands showed two increases (Fig. 7) that took place after the first nutrient addition (day 1) and the rain event (day 17).

Whatever their specific biological source, it is somewhat puzzling why two separate ligands,  $L_1$  and  $L_2$ , were necessary to produce the buffering effect and how the biological processes producing these ligands could be so well tuned as to maintain the sum  $C_{L1} + C_{L2}$  relatively well matched to  $[Cu_{diss}]$ . Perhaps a more straightforward explanation is that  $L_1$  and  $L_2$  are one and the same ligand and that the very high-affinity signature ( $15.2 < \log K'_1 < 16.0$ ) observed in the CLE-ASV titrations arises when the  $L_2$  ligand becomes entrapped within a colloidal matrix. When/if this happened, the  $L_2$  ligand—together with the bound Cu—would no longer be readily accessible, so that a much higher concentration of EN would be required to titrate it. Thus,  $CuL_2$  complexes buried deep inside colloids could appear to be much stronger than their counterparts in solution. In such a scenario, the term colloid refers to entities large enough to acquire an interface (i.e., the interior has different physicochemical properties from the surrounding medium) but small enough to be included with the dissolved phase upon filtration through 0.40- $\mu$ m membrane filters. A situation whereby the rates of complex formation/dissociation were different when ligands were bound to the colloidal phase, compared with the truly dissolved phase, has actually been reported for Pb in the Firth of Clyde (Muller 1998). A similar situation for Cu-binding ligands could have occurred in the waters of the Raunefjord. If so, it would explain why the steady decrease (77–42%) in the percentage of Cu present as  $CuL_2$  between days 5 and 15 was mirrored by a steady increase (23–55%) in  $CuL_1$ , as more colloidal matter was being

Table 5. Dissolved, labile, and free Zn concentrations, Zn-binding ligand concentrations, and related conditional stability constants measured during the course of the mesocosm experiment.

Day	[Zn <sub>diss.</sub> ] (nmol L <sup>-1</sup> )	α-inorg	(nmol L <sup>-1</sup> )			
			[Zn <sub>labile</sub> ]	[Zn <sup>2+</sup> ]	C <sub>L1</sub>	log K <sub>1</sub>
Bag 8, depth = 2 m						
1	33.1	1.9	9.3	4.87	37	8.57
3	35.5	1.9	11.7	6.14	36	8.40
5	29.1	2.0	11.0	5.51	30	8.44
7	22.3	2.0	6.6	3.28	27	8.63
9	24.8	2.0	2.7	1.33	90	8.39
11	22.7	2.1	1.8	0.85	212	8.11
13	25.2	2.1	1.3	0.61	156	8.47
15	20.0	2.1	0.9	0.41	121	8.66
17	33.7	1.9	1.6	0.86	135	8.56
19	27.0	2.0	0.9	0.48	117	8.78
21	29.9	2.1	1.8	0.90	117	8.60
Bag 9, depth = 2 m						
1	32.0	1.9	12.2	6.44	32	8.40
3	36.1	1.9	12.6	6.63	39	8.36
5	29.2	1.9	12.2	6.40	23	8.65
7	24.3	2.0	8.2	4.09	24	8.70
9	19.8	2.0	3.6	1.81	63	8.28
11	15.5	2.0	1.1	0.54	148	8.36
13	19.1	2.0	1.0	0.50	126	8.53
15	20.0	2.1	0.7	0.33	135	8.70
17	31.3	1.9	1.4	0.74	120	8.65
19	27.0	2.1	1.2	0.59	98	8.78
21	25.7	2.1	2.1	1.03	86	8.71
Bag 10, depth = 2 m						
1	35.2	1.9	10.1	5.30	36	8.64
3	33.9	1.9	11.1	5.86	33	8.58
5	31.4	2.0	9.9	4.94	30	8.71
7	27.0	2.0	6.5	3.27	27	8.98
9	27.0	2.0	3.5	1.74	84	8.35
11	21.5	2.0	1.4	0.68	125	8.45
13	25.6	2.0	2.0	1.00	132	8.34
15	29.0	2.0	1.8	0.91	104	8.59
17	39.7	1.9	2.3	1.20	112	8.62
19	34.0	2.0	1.3	0.67	122	8.74
21	31.8	2.1	1.9	0.94	105	8.79
Raunefjord, depth = 5 m						
7	23.9	2.0	1.9	0.97	37	9.18
11	24.2	2.0	1.8	0.92	101	8.49
15	17.3	2.1	0.6	0.27	163	8.62
19	28.8	2.1	0.7	0.34	170	8.77

formed during that period. This colloid issue remains to be settled, however (for example, through studies involving ultrafiltration or field-flow fractionation techniques).

*Sources and potential ecological role of the weak Cu-binding and Zn-binding ligands*—As discussed above, [Cu<sup>2+</sup>] was reduced to much lower levels during the August study (this work) than during the June study (Muller et al. 2003) due to the formation of very strong complexes that bound 80–99.8% of dissolved Cu in August compared to only 20–60% in June. Since the water temperature was 20°C in August (this study) and 10°C in June (Muller et al. 2003), this finding is consistent with the temperature-related sea-

sonal appearance of strong ligands already noted by Croot (2003) in the Gullmar Fjord. In addition, a recent study conducted in the Raunefjord from February to April revealed that *Synechococcus* cell numbers tended to be elevated (though they never exceeded  $3 \times 10^3$  cells mL<sup>-1</sup>) immediately after major blooms of diatoms (Larsen et al. 2004). Temporarily higher *Synechococcus* cell numbers under those conditions could be due to the release of weak Cu-binding ligands produced as metabolic or decomposition products of diatoms. The concentration of weak Cu-binding ligands, C<sub>L3</sub>, measured in the bags increased dramatically during and up to 4 d following the exponential growth phase of *Synechococcus* sp., nanoeukaryotes, and diatoms (Figs. 3, 4). The

Table 6. Dissolved, labile, and free Mn concentrations, Mn-binding ligand concentrations, and apparent conditional stability constants measured during the course of the mesocosm experiments.

Day	[Mn <sub>diss.</sub> ] (nmol L <sup>-1</sup> )	$\alpha$ -inorg	(nmol L <sup>-1</sup> )			log $K'_1$
			[Mn <sub>labile</sub> ]	[Mn <sup>2+</sup> ]	C <sub>L1</sub>	
Bag 8, depth = 2 m						
1	26.6	1.16	15.3	13.2	12.9	8.74
3	28.0	1.17	17.0	14.5	12.5	8.70
5	25.0	1.17	10.6	9.1	16.0	9.00
7	19.8	1.16	3.6	3.1	22.1	8.94
9	20.0	1.17	3.1	2.6	22.5	9.08
11	14.6	1.18	5.5	4.7	11.2	8.97
13	14.4	1.18	4.9	4.2	11.2	9.10
15	16.1	1.19	3.7	3.1	16.7	8.96
17	22.0	1.16	8.9	7.7	14.6	9.02
19	19.1	1.17	7.7	6.6	13.7	8.89
21	18.6	1.17	9.8	8.4	10.0	8.94
Bag 9, depth = 2 m						
1	24.8	1.16	13.9	12.0	12.2	8.81
3	26.1	1.17	14.1	12.1	12.7	9.07
5	25.0	1.17	8.0	6.8	19.6	8.95
7	22.0	1.18	3.6	3.0	23.6	9.07
9	20.8	1.18	2.9	2.5	25.2	8.99
11	16.0	1.18	3.6	3.1	15.5	9.11
13	13.9	1.19	6.1	5.1	9.1	9.05
15	13.8	1.20	2.4	2.0	17.5	8.96
17	18.5	1.18	5.2	4.4	17.0	8.92
19	17.0	1.18	4.0	3.4	19.3	8.78
21	17.7	1.18	4.3	3.7	16.6	9.06
Bag 10, depth = 2 m						
1	27.0	1.17	14.2	12.1	14.0	8.98
3	29.0	1.17	17.2	14.7	12.5	9.02
5	26.6	1.18	12.5	10.6	15.2	9.07
7	21.7	1.19	3.0	2.5	25.7	9.03
9	21.0	1.19	2.5	2.1	27.9	8.91
11	13.1	1.19	3.9	3.3	11.9	9.01
13	15.0	1.19	7.6	6.4	8.6	8.98
15	15.0	1.20	4.6	3.8	13.2	9.00
17	23.3	1.19	10.1	8.5	14.4	9.10
19	20.0	1.19	6.8	5.7	16.3	8.89
21	19.0	1.19	8.4	7.0	13.0	8.80
Raunefjord, depth = 5 m						
7	19.3	1.18	2.8	2.3	23.3	9.03
11	17.0	1.18	4.3	3.6	15.2	9.15
15	17.5	1.20	6.3	5.2	13.0	9.09
19	20.0	1.20	5.2	4.3	18.5	8.98

squares of the correlation coefficient of C<sub>L3</sub> versus the respective algal group abundances between days 1 and 11 were 0.54, 0.76, and 0.40. During this period, C<sub>L3</sub> also showed a correlation ( $r^2 = 0.75$ ,  $n = 16$ ) to the Chl *a* values and, more significantly ( $r^2 = 0.90$ ,  $n = 19$ , including fjord data), to the proteinlike DOM fluorescence (Fig. 8). However, none of these relations held for the rest of the experiment. It seems reasonable to conclude, therefore, that the proteinlike fluorescence material (including both tyrosine-like and tryptophan-like compounds) and the pool of L<sub>3</sub> ligands were not one and the same, but that they had the same source or production process, which, in turn, was related to algal growth.

Zn-binding ligands forming relatively weak complexes ( $\log K'_1 = 8.56 \pm 0.18$ ) were present at levels <40 nmol L<sup>-1</sup> until day 7; thereafter, their concentrations increased to 130–210 nmol L<sup>-1</sup> on day 11 and then leveled off at 90–130 nmol L<sup>-1</sup> from day 15 onward (Fig. 5). In sharp contrast with all other ligands detected, Zn-C<sub>L1</sub> showed no significant change during the exponential growth phase of algae. In fact, it increased dramatically at the start of the “stationary” phase of algal growth, between days 7 and 11, coinciding with a decrease in Chl *a* (Fig. 2). This observation is consistent with those from other investigations (Ellwood and van den Berg 2000; Muller et al. 2001, 2003) in suggesting that the Zn-binding ligands are released by destructive pro-

cesses such as the bacterial decomposition of algal cells or consumption by grazers. Bacterial decomposition does not seem to be the most likely scenario, as there was no obvious correlation between Zn- $C_{L1}$  and heterotrophic bacterial abundance. Furthermore, Zn- $C_{L1}$  reached its highest value in bag 8, whereas cell counts at the height of algal or bacterial blooms were systematically highest in bag 10. The grazing process was not investigated in the present study and would clearly need to be considered in future studies of Zn speciation.

*Chemical and biological perturbations caused by the rain event*—The immediate effect of the rain event was the mixing of 11 m<sup>3</sup> of seawater with 0.23 m<sup>3</sup> of rainwater. Inputs of fjord water during the 8-h precipitation period can be neglected as a first approximation. This approximation can be verified to be valid by estimating the volume of rainwater added to each of the bags from the change in salinity: we found 0.24, 0.20, and 0.20 m<sup>3</sup> for bags 8, 9, and 10, respectively. The total metal concentrations in rainwater (rw) can thus be calculated from simple mole balance equations describing the mixing of the two waters. From this calculation, repeated for each of the bags, we obtain [Cu<sub>rw</sub>] = 130 ± 70 nmol L<sup>-1</sup>, [Zn<sub>rw</sub>] = 760 ± 110 nmol L<sup>-1</sup>, and [Mn<sub>rw</sub>] = 880 ± 120 nmol L<sup>-1</sup>. These values are 3–15 times higher than the concentrations of metals in rainwater collected in areas of the North Sea under conditions of both westerly and southeasterly flow (Spokes et al. 2001). Moreover, the Mn:Zn molar ratio recorded (1.16 ± 0.24) was much higher than that (Mn:Zn = 0.38 ± 0.12) recorded by Spokes et al. (2001) in wet deposition over the northeast Atlantic Ocean after the air had passed over the most heavily populated and industrialized regions of Europe. Lastly, the Cu:Zn molar ratio recorded (0.16 ± 0.08) was identical to that (Cu:Zn = 0.19 ± 0.07) measured in surface soils across four areas of southwestern and southern Norway (Steinnes et al. 1997). This leaves very little doubt that the main source of the metals added to the bags on day 17 was an airborne supply of soil material from southern Norway. This view is consistent with the high-pressure conditions experienced over Scandinavia during the preceding 3 weeks. Rather unexpectedly, a large percentage of the metal load supplied by the deposition event disappeared from the water column in the following 2 d: 140% (±10%) for Cu, 50% (±18%) for Zn, and 77% (±15%) for Mn.

The short-term (days 17–19) ecological impact of the rain event was an enhancement of diatom cell densities but a decrease in the densities of bacterial cells, especially for cyanobacteria. Thus, diatom cell densities increased sharply to reach their highest level 1 d after the event (Fig. 3). By contrast, *Synechococcus* sp. numbers (Fig. 3) decreased, slowly at first, to reach their lowest level 2–3 d after the event. There is at least one documented example of rainfall stimulation of primary production at both coastal and offshore locations (Paerl et al. 1999) that was attributed to the supply of inorganic N and colimiting micronutrients (e.g., Fe). In our experiment, also, the rain was likely a source of dissolved N (Table 1) and micronutrients (Tables 4–6) to the bags and fjord. Before the event, the biomass in bags 8–10 and in the excess-N bags (data not shown) followed the pat-

tern 6 > 7 > 8, 9, 10. Given that the daily N additions to bags 6 and 7 were 4 and 2 times those made to bags 8–10, the N pulse delivered by rain would likely have stimulated primary production in bags 8–10.

The fates of the metals delivered by the rain showed significant differences. For instance, 2 d after the rainfall perturbation, both labile and total dissolved portions of Zn and Mn were still elevated compared with their values before the perturbation (Figs. 5, 6). By contrast, both [Cu<sub>diss</sub>] and [Cu<sub>labile</sub>] had dropped to values lower than those recorded before the perturbation. This counterintuitive result can be understood if we consider the involvement of the biota in the production and release of strong Cu-binding ligands. The Cu pulse due to rainfall appears to have stimulated the active release of L<sub>2</sub> ligands (Fig. 4), possibly to counteract the toxic effects of Cu to smaller cells such as cyanobacteria. During the same period (days 17–19), a net decrease in the concentration of L<sub>1</sub> ligands was observed in each of the bags, although this was matched by a greater or equal decrease in the concentration of Cu (Table 4; Fig. 4). Taken collectively, these observations conform to what would be expected if the L<sub>2</sub> ligands released in solution to counteract the toxic effects of Cu<sup>2+</sup> were in equilibrium with a colloidal matrix (L<sub>1</sub>), which ultimately reached a size and density that would cause it to sink—and thus remove CuL<sub>1</sub>—to the bottom of the bags.

## References

- BRÜGMANN, L., AND J. KUSS. 1999. Analysis of marine particles, p. 345–359. In K. Grasshoff, K. Kremling, and M. Ehrardt [eds.], *Methods of seawater analysis*. Wiley-VCH.
- COBLE, P. G. 1996. Characterization of marine and terrestrial DOM in seawater using excitation–emission matrix spectroscopy. *Mar. Chem.* **51**: 325–346.
- CROOT, P. L. 2003. Seasonal cycle of copper speciation in Gullmar Fjord, Sweden. *Limnol. Oceanogr.* **48**: 764–776.
- , J. W. MOFFETT, AND L. E. BRAND. 2000. Production of extracellular Cu complexing ligands by eukaryotic phytoplankton in response to Cu stress. *Limnol. Oceanogr.* **45**: 619–627.
- DETERMANN, S., J. M. LOBBES, R. REUTER, AND J. RULLKOTTER. 1998. Ultraviolet fluorescence excitation and emission spectroscopy of marine algae and bacteria. *Mar. Chem.* **62**: 137–156.
- , R. REUTER, P. WANGER, AND R. WILLKOMM. 1994. Fluorescent matter in the eastern Atlantic Ocean. Part 2: Vertical profiles and relation to water masses. *Deep-Sea Res.* **43**: 345–360.
- DUPONT, C. L., R. K. NELSON, S. BASHIR, J. W. MOFFETT, AND B. A. AHNER. 2004. Novel copper-binding and nitrogen-rich thiols produced and exuded by *Emiliania huxleyi*. *Limnol. Oceanogr.* **49**: 1754–1762.
- EGGE, J. K., AND D. L. AKSNES. 1992. Silicate as regulating nutrient in phytoplankton competition. *Mar. Ecol. Prog. Ser.* **83**: 281–289.
- ELLWOOD, M. J., AND C. M. G. VAN DEN BERG. 2000. Zinc speciation in the northeastern Atlantic Ocean. *Mar. Chem.* **68**: 295–306.
- HELDAL, M., K. M. FAGERBAKKE, P. TUOMI, AND G. BRATBAK. 1996. Abundant populations of iron and manganese sequestering bacteria in coastal water. *Aquat. Microb. Ecol.* **11**: 127–133.
- HUDSON, R. J. M., AND F. M. M. MOREL. 1993. Trace metal trans-

- port by marine organisms: Implications of metal coordination kinetics. *Deep-Sea Res. I* **40**: 129–150.
- JACQUET, S., M. HELDAL, D. IGLESIAS-RODRIGEZ, A. LARSEN, W. H. WILSON, AND G. BRATBAK. 2002. Flow cytometric analysis of an *Emiliania huxleyi* bloom terminated by viral infection. *Aquat. Microb. Ecol.* **27**: 111–124.
- KESTER, D. R. 1986. Equilibrium models in seawater: Applications and limitations, p. 337–363. *In* M. Bernhard, F. E. Brinckman, and P. J. Sadler [eds.], The importance of chemical speciation in environmental processes. Dahlem Konferenzen 1986. Springer.
- LARSEN, A., AND OTHERS. 2001. Population dynamics and diversity of phytoplankton, bacteria and virus in a seawater enclosure. *Mar. Ecol. Prog. Ser.* **221**: 47–57.
- AND ———. 2004. Spring phytoplankton bloom dynamics in Norwegian coastal waters: Microbial community succession and diversity. *Limnol. Oceanogr.* **49**: 180–190.
- LUTHER, G. W., D. B. NUZZIO, AND J. F. WU. 1994. Speciation of manganese in Chesapeake Bay by voltammetric methods. *Anal. Chim. Acta* **284**: 473–480.
- MARIE, D., C. P. D. BRUSSARD, R. THYRHAUG, G. BRATBAK, AND D. VAULOT. 1999. Enumeration of marine viruses in culture and natural samples by flow cytometry. *Appl. Environ. Microbiol.* **65**: 45–52.
- MOFFETT, J. W., AND L. E. BRAND. 1996. Production of strong, extracellular Cu chelators by marine cyanobacteria in response to Cu stress. *Limnol. Oceanogr.* **41**: 388–395.
- , ———, P. L. CROOT, AND K. A. BARBEAU. 1997. Cu speciation and cyanobacterial distribution in harbors subject to anthropogenic Cu inputs. *Limnol. Oceanogr.* **42**: 789–799.
- MULLER, F. L. L. 1998. Colloid/solution partitioning of metal-selective organic ligands and its relevance to Cu, Pb and Cd cycling in the Firth of Clyde. *Estuarine Coastal Shelf Sci.* **46**: 419–437.
- , S. B. GULIN, AND Å. KALVØY. 2001. Chemical speciation of copper and zinc in surface waters of the western Black Sea. *Mar. Chem.* **76**: 233–251.
- , S. JACQUET, AND W. H. WILSON. 2003. Biological factors regulating the chemical speciation of Cu, Zn, and Mn under different nutrient regimes in a marine mesocosm experiment. *Limnol. Oceanogr.* **48**: 2289–2302.
- PAERL, H. W., J. D. WILLEY, M. GO, B. L. PEIERLS, J. L. PINCKNEY, AND M. L. FOGEL. 1999. Rainfall stimulation of primary production in western Atlantic Ocean waters: Roles of different nitrogen sources and co-limiting nutrients. *Mar. Ecol. Prog. Ser.* **176**: 205–214.
- PARLANTI, E., K. WÖRZ, L. GEOFFROY, AND M. LAMOTTE. 2000. Dissolved organic matter fluorescence spectroscopy as a tool to estimate biological activity in a coastal zone submitted to anthropogenic inputs. *Org. Geochem.* **31**: 1765–1781.
- RIEBESELL, U., AND D. A. WOLF-GLADROW. 2002. Supply and uptake of inorganic nutrients, p. 109–140. *In* P. J. le B. Williams, D. N. Thomas, and C. S. Reynolds [eds.], Phytoplankton productivity. Blackwell.
- ROCHELLE-NEWALL, E. J., AND T. R. FISHER. 2002. Production of chromophoric dissolved organic matter fluorescence in marine and estuarine environments: An investigation into the role of phytoplankton. *Mar. Chem.* **77**: 7–21.
- ROITZ, J. S., AND K. W. BRULAND. 1997. Determination of dissolved manganese(II) in coastal and estuarine waters by differential pulse cathodic stripping voltammetry. *Anal. Chim. Acta* **344**: 175–180.
- RUŽIĆ, I. 1982. Theoretical aspects of the direct titration of natural waters and its information yield for trace metal speciation. *Anal. Chim. Acta* **140**: 99–113.
- SCARANO, G., E. BRAMANTI, AND A. ZIRINO. 1992. Determination of copper complexation in seawater by a ligand competition technique with voltammetric measurement of the labile fraction. *Anal. Chim. Acta* **264**: 153–162.
- SCHECHER, W. D., AND D. C. MCAVOY. 1998. MINEQ+: Chemical equilibrium modeling system, version 4.0 for Windows. Environmental Research Software.
- SPOKES, L., T. JICKELLS, AND K. JARVIS. 2001. Atmospheric inputs of trace metals to the northeast Atlantic Ocean: The importance of the southeasterly flow. *Mar. Chem.* **76**: 319–330.
- STEDMON, C. A., S. MARKAGER, AND R. BRO. 2003. Tracing dissolved organic matter in aquatic environments using a new approach to fluorescence spectroscopy. *Mar. Chem.* **82**: 239–254.
- STEINNES, E., R. O. ALLEN, H. M. PETERSEN, J. P. RAMBÆK, AND P. VARSKOG. 1997. Evidence of large scale heavy metal contamination of natural surface soils in Norway from long-range atmospheric transport. *Sci. Total Environ.* **205**: 255–266.
- SUNDA, W. G., AND S. A. HUNTSMAN. 1994. Photoreduction of manganese oxides in seawater. *Mar. Chem.* **46**: 133–152.
- VASCONCELOS, M.T.S.D., M. F. C. LEAL, AND C. M. G. VAN DEN BERG. 2002. Influence of the nature of the exudates released by different marine algae on the growth, trace metal uptake and exudation of *Emiliania huxleyi* in natural seawater. *Mar. Chem.* **77**: 187–210.
- WHITFIELD, M. 2001. Interactions between phytoplankton and trace metals in the ocean. *Adv. Mar. Biol.* **41**: 1–128.
- YAMASHITA, Y., AND E. TANOUE. 2003. Distribution and alteration of amino acids in bulk DOM along a transect from bay to oceanic waters. *Mar. Chem.* **82**: 145–160.

Received: 6 July 2004

Amended: 31 May 2005

Accepted: 5 June 2005